Simultaneous two-dimensional phononic and photonic band gaps in opto-mechanical crystal slabs

Saeed Mohammadi[1*], Ali A. Eftekhar[1], Abdelkrim Khelif[2, 3], and Ali Adibi[1]

[1]*School of Electrical and Computer Engineering, Georgia Institute of Technology, Atlanta, GA 30332, USA*
[2]*International joint laboratory Georgia Tech-CNRS UMI; 2-3 Rue Marconi 57070 Metz, France*
[3]*Institut FEMTO-ST, CNRS; 32 avenue de l'Observatoire 25044 Besancon Cedex, France*
**saeedm@gatech.edu*

Abstract: We demonstrate planar structures that can provide simultaneous two-dimensional phononic and photonic band gaps in opto-mechanical (or phoxonic) crystal slabs. Different phoxonic crystal (PxC) structures, composed of square, hexagonal (honeycomb), or triangular arrays of void cylindrical holes embedded in silicon (Si) slabs with a finite thickness, are investigated. Photonic band gap (PtBG) maps and the complete phononic band gap (PnBG) maps of PxC slabs with different radii of the holes and thicknesses of the slabs are calculated using a three-dimensional plane wave expansion code. Simultaneous phononic and photonic band gaps with band gap to midgap ratios of more than 10% are shown to be readily obtainable with practical geometries in both square and hexagonal lattices, but not for the triangular lattice.

OCIS codes: (160.5293) Photonic bandgap materials; (120.4880) Opto-mechanics; (050.5298) Photonic crystals

References and links

1. E. Yablonovitch, T. Gmitter, and K. Leung, "Inhibited spontaneous emission in solid-state physics and electronics," Phys. Rev. Lett. **58**(20), 2059–2062 (1987).
2. M. Loncar, D. Nedeljkovi, T. Doll, J. Vuckovic, A. Scherer, and T. P. Pearsall, "Waveguiding in planar photonic crystals," Appl. Phys. Lett. **77**(13), 1937–1939 (2000).
3. Y. Akahane, T. Asano, B. S. Song, and S. Noda, "High-Q photonic nanocavity in a two-dimensional photonic crystal," Nature **425**(6961), 944–947 (2003).
4. M. Koshiba, "Wavelength division multiplexing and demultiplexing with photonic crystal waveguide couplers," J. Lightwave Technol. **19**(12), 1970–1975 (2001).
5. M. M. Sigalas, and E. N. Economou, "Elastic and Acoustic-Wave Band-Structure," J. Sound Vibrat. **158**(2), 377–382 (1992).
6. T. Carmon, H. Rokhsari, L. Yang, T. J. Kippenberg, and K. J. Vahala, "Temporal behavior of radiation-pressure-induced vibrations of an optical microcavity phonon mode," Phys. Rev. Lett. **94**(22), 223902 (2005).
7. M. Eichenfield, R. Camacho, J. Chan, K. J. Vahala, and O. Painter, "A picogram- and nanometre-scale photonic-crystal optomechanical cavity," Nature **459**(7246), 550–555 (2009).
8. A. V. Akimov, Y. Tanaka, A. B. Pevtsov, S. F. Kaplan, V. G. Golubev, S. Tamura, D. R. Yakovlev, and M. Bayer, "Hypersonic modulation of light in three-dimensional photonic and phononic band-gap materials," Phys. Rev. Lett. **101**(3), 033902–033905 (2008).
9. P. Dainese, P. S. J. Russell, N. Joly, J. C. Knight, G. S. Wiederhecker, H. L. Fragnito, V. Laude, and A. Khelif, "Stimulated Brillouin scattering from multi-GHz-guided acoustic phonons in nanostructured photonic crystal fibres," Nat. Phys. **2**(6), 388–392 (2006).
10. M. Maldovan, and E. L. Thomas, "Simultaneous complete elastic and electromagnetic band gaps in periodic structures," Appl. Phys. B **83**(4), 595–600 (2006).
11. M. Maldovan, and E. L. Thomas, "Simultaneous localization of photons and phonons in two-dimensional periodic structures," Appl. Phys. Lett. **88**(25), 251907 (2006).
12. S. Sadat-Saleh, S. Benchabane, F. I. Baida, M. P. Bernal, and V. Laude, "Tailoring simultaneous photonic and phononic band gaps," J. Appl. Phys. **106**(7), 074912 (2009).
13. A. Khelif, B. Aoubiza, S. Mohammadi, A. Adibi, and V. Laude, "Complete band gaps in two-dimensional phononic crystal slabs," Phys. Rev. E Stat. Nonlin. Soft Matter Phys. **74**(4), 046610 (2006).

#123986 - $15.00 USD Received 9 Feb 2010; revised 5 Apr 2010; accepted 7 Apr 2010; published 16 Apr 2010

14. S. Mohammadi, A. A. Eftekhar, A. Khelif, H. Moubchir, R. Westafer, W. D. Hunt, and A. Adibi, "Complete phononic bandgaps and bandgap maps in two-dimensional silicon phononic crystal plates," Electron. Lett. **43**(16), 898–899 (2007).
15. S. Mohammadi, A. A. Eftekhar, A. Khelif, W. D. Hunt, and A. Adibi, "Evidence of large high frequency complete phononic band gaps in silicon phononic crystal plates," Appl. Phys. Lett. **92**(22), 221905 (2008).
16. S. Mohammadi, A. A. Eftekhar, W. D. Hunt, and A. Adibi, "Demonstration of large complete phononic band gaps and waveguiding in high-frequency silicon phononic crystal slabs," in Proceedings of *2008 IEEE International Frequency Control Symposium,* 2008 IEEE International Frequency Control Symposium, FCS (IEEE, 2008), 768–772.
17. R. H. Olsson III, I. F. El-Kady, M. F. Su, M. R. Tuck, and J. G. Fleming, "Microfabricated VHF acoustic crystals and waveguides," Sens. Actuators A Phys. **145-146**, 87–93 (2008).
18. S. Mohammadi, A. A. Eftekhar, W. D. Hunt, and A. Adibi, "High-Q micromechanical resonators in a two-dimensional phononic crystal slab," Appl. Phys. Lett. **94**, 051906–1 (2009).
19. K. M. Ho, C. T. Chan, and C. M. Soukoulis, "Existence of a photonic gap in periodic dielectric structures," Phys. Rev. Lett. **65**(25), 3152–3155 (1990).
20. M. Kushwaha, P. Halevi, G. Martinez, L. Dobrzynski, and B. Djafari-Rouhani, "Theory of acoustic band structure of periodic elastic composites," Phys. Rev. B **49**(4), 2313–2322 (1994).
21. S. G. Johnson, S. H. Fan, P. R. Villeneuve, J. D. Joannopoulos, and L. A. Kolodziejski, "Guided modes in photonic crystal slabs," Phys. Rev. B **60**(8), 5751–5758 (1999).
22. W. Axmann, and P. Kuchment, "An efficient finite element method for computing spectra of photonic and acoustic band-gap materials I. Scalar case," J. Comput. Phys. **150**(2), 468–481 (1999).
23. L. Andreani, and M. Agio, "Photonic bands and gap maps in a photonic crystal slab," IEEE J. Quantum Electron. **38**(7), 891–898 (2002).

1. Introduction

Waves propagating in structures with periodicities of the order of their wavelength can undergo dispersive effects that are not obtainable in conventional bulk materials. Exemplarily, photonic crystals, which are structures with periodic changes in their photonic properties (e.g., dielectric permittivity, can potentially have photonic band gaps (PtBGs) [1]. PtBGs are frequency ranges in which the propagation of photons is prohibited. PtBGs in PtCs can be used to efficiently guide, trap, and confine optical energy in small volumes. This has enabled realizing compact and efficient devices such as PtC waveguides [2], resonators [3], and wavelength multiplexers/de-multiplexers [4].

Similarly, phononic band gaps (PnBGs) [5] are ranges of frequencies in which elastic waves (or phonons) are not allowed to propagate. PnBGs can be obtained in phononic crystals (PnCs), which are carefully designed structures with periodic variation in their mechanical (or acoustic) properties (such as elastic constant or mass density). Analog to PtCs, PnCs can be used to effectively confine elastic (or acoustic) energy and therefore, enable realization of phononic devices with improved performances compared to their conventional counterparts.

Because of the high levels of energy confinement that they can provide, obtaining PnBG and PtBGs simultaneously in optically and acoustically-periodic structures, dubbed opto-mechanical or phoxonic crystals (PxCs) is of great interest. PxCs with simultaneous PnBGs and PtBGs can be used to enhance opto-mechanical [6] and acousto-optic interactions. Such enhancements have already been observed for one-dimensionally-periodic PxC slabs [7] three-dimensional (3D) PxCs [8], and PxC fibers [9]. Therefore, the ability to obtain such high levels of confinement in two dimensions through the use of PnBGs and PtBGs in practical structures compatible with planar fabrication technology should be of great benefit for obtaining such functionalities in a more compact and efficient platform.

Maldovan and Thomas have recently shown theoretically, that simultaneous two-dimensional (2D) PnBGs and PtBGs exist for waves propagating in the plane of periodicity (or in-plane waves) in PxCs of infinitely long void cylindrical inclusions in silicon (Si) [10]. Both square and triangular arrangements of the inclusions were considered. They also have theoretically shown that the photonic and phononic energies can be simultaneously localized in such PxC structures with defects [11]. In addition, maps of simultaneous PnBGs and PtBGs for a similar structure in $LiNbO_3$ with optimization of the size of the gap have been recently reported [12]. However, all of the considered structures in these studies have been assumed to

#123986 - $15.00 USD Received 9 Feb 2010; revised 5 Apr 2010; accepted 7 Apr 2010; published 16 Apr 2010

be infinite (or very large compared to the wavelength) and the fields are assumed invariant in the third dimension

Among practical planar PnC structures with potential PnBGs, PnC slabs (structures with periodicity within a plane and with a finite thickness of the order of wavelength in the third dimension) [13, 14, 15] have unique advantages for realization of fundamental building blocks of micro/nano-mechanical signal processing components such as waveguides [16, 17] and resonators [18]. Interest in PnC slab structures is mainly due to their low loss as the energy can be well confined within the thickness of the slab. Moreover, PtC slabs with PtBGs have been used to effectively control the propagation of photonic waves and form efficient photonic waveguides [2] and resonators [3]. Among possible slab architectures, PnC and PtC slab structures with void holes in a solid background [2, 3, 14-16, 18] are advantageous over the ones with composite lattices [13, 17] due to the lower cost of fabrication and the possibility of full realization using single-crystalline solids (that will eventually translate to lower mechanical and photonic losses). Therefore, obtaining simultaneous band gaps for phonons and photons in these PxC slabs can be of great interest. It should also be noted that in many cases, the photonic and phononic properties of such practically realizable structures can be completely different from those of the structures with infinite thickness as in Refs. [10-12].

In this paper, we show that simultaneous 2D PtBGs and complete 2D PnBGs can be simultaneously obtained in PxC slabs made of void (vacuum or air) cylindrical holes embedded in a free-standing solid slab. We show that the band structure and in-plane PnBGs and PtBGs of such PxCs slabs can be drastically different compared to PxCs of the same structure but with infinite thickness. We also show the possibility of engineering and optimizing these simultaneous band gaps by using the geometrical parameters (e.g., radius of the inclusions and thickness of the slab) of the PxC slab structures. While the results of this study can be applicable to many solid materials, we limit our study to Si due to its technological advantages and for definiteness. We expect that by using the results presented in this paper, opto-mechanical devices with better control over the phononic and photonic energies, better performance characteristics, and smaller form factors can be obtained.

2. Method of simulation and simulation assumptions

To calculate the photonic and phononic band structures of the PxCs, we have developed and used a plane wave expansion (PWE) tool [19, 20]. In order to find the photonic band structure using PWE, we can simplify the Maxwell's equations to

$$\nabla \times \left[\frac{1}{\varepsilon} \nabla \times H \right] = \frac{\omega^2}{c^2} H, \tag{1}$$

where ε is the position-dependent dielectric permittivity and H is the magnetic field intensity vector. Equation (1) is then converted to an eigenvalue problem by expanding the magnetic field intensity using a plane wave basis and the dielectric permittivity using Fourier transform [19].

For simulating structures with infinite thickness in the third dimension, it is assumed that the field values are independent of the changes in the third dimension and therefore, the computations are significantly simplified. The number of plane waves used is of the order of 100, which ensures the accuracy of the results.

For the PxC slab structures, we have assumed 2D periodicity in the slab plane and a periodic sequence of slabs separated by a sufficiently long distance in the third dimension to ensure minimum interaction of the guided slab modes [21]. The non-guided (radiation) modes, which fall within the light cone, are ignored in this procedure, however, these modes are of limited interest as they cannot be confined within the slab and are radiated away. Enough number of plane waves (of the order of 800) is used to ensure the convergence accuracy of the results.

#123986 - $15.00 USD Received 9 Feb 2010; revised 5 Apr 2010; accepted 7 Apr 2010; published 16 Apr 2010

In order to calculate the phononic bands using PWE, we implemented a similar procedure [20] by simplifying Newton's law and the elastic constitutive relation to the form

$$\nabla \cdot (\mathbf{c} \cdot \nabla_s \mathbf{u}) = -\rho\omega^2 \mathbf{u}, \tag{2}$$

in which **c** and ρ are the position-dependent stiffness tensor and mass density, respectively and **u** is the displacement vector. As can be seen by comparing Eqs. (1) and (2), these equations share many similarities. However, in the phononic case, the distance between the periodically placed slabs in the slab thickness direction is not as critical as for the photonic case since the modes are strictly confined within the freestanding slab structure. Nevertheless, the number of plane waves we used for the phononic case is also of the same order (i.e., 800) to ensure the accuracy. The results are also in excellent agreement with our calculations using the finite element method [22] in all test cases.

Using the photonic and phononic PWE tools, we performed both 3D and 2D simulations for structures with finite and infinite thicknesses, respectively. Throughout this paper, Si is assumed to be crystalline with its main symmetry axes aligned to *x*, *y*, and *z* directions of the coordinate system. The anisotropy of the mechanical parameters of the Si is fully considered in our simulations. The material parameters of Si are assumed to be $\varepsilon_r = 12.25$, $c_{11} = 16.7 \times 10^{10}$ N/m^2, $c_{12} = 6.39 \times 10^{10}$ N/m^2, $c_{44} = 7.956 \times 10^{10}$ N/m^2, and $\rho = 2332$ kg/m^3, where ε_r is the relative permittivity, c_{11}, c_{12}, c_{44} are the independent components of the stiffness tensor, and ρ is the mass density of Si.

3. Comparison of the band structures of 2D PxCs and PxC slabs

Figure 1(a) shows the band structure of elastic waves propagating in the plane of periodicity (or in-plane waves) in a 2D square-lattice array of infinitely long void holes in a Si background calculated using the 2D PWE. A schematic of the cross section of such PxC is shown in the inset of Fig. 1(a). In this figure, *a* is the spacing between the centers of the nearest holes (or the lattice constant) and *r* is the radius of the holes. The normalized radius of the holes is $r/a = 0.45$. As can be seen in Fig. 1(a), a PnBG exists in this PxC and covers a frequency range of 2430 m/s < $f \times a$ < 3619 m/s. Figure 1(b) shows the band structure of elastic waves in a square-lattice Si PxC slab calculated using 3D PWE. A schematic of the structure is shown in the inset of Fig. 1(b), where *a* is the lattice constant, *r* is the radius of the holes, and *d* is the thickness of the slab. The normalized radius of the holes in the structure is the same as that of the structure in Fig. 1(a) (i.e., $r/a = 0.45$), and the normalized thickness of the structure is $d/a = 0.5$ rather than infinite. The PnBG for this structure extends in the frequency range of 3000 m/s < $f \times a$ < 3260 m/s. As can be seen, the band structure and the PnBG of the structure with a finite thickness [shown in Fig. 1(b)] are considerably different from those of the structure with infinite thickness [shown in Fig. 1(a)].

We performed the same analysis for photonic waves in the same square-lattice PxCs of Fig. 1(a) and Fig. 1(b) by calculating their photonic band structure. The 2D photonic band structure of the in-plane transverse electric (TE) modes (electric field in the plane of propagation) and the transverse magnetic (TM) modes (magnetic field in the plane of propagation) for the structure of Fig. 1(a) are shown in Fig. 1(c). The normalized radius of the holes is $r/a = 0.45$ as in the case of Fig. 1(a). As can be seen in Fig. 1(c), there are both TE and TM PtBGs in the photonic band structure.

For the case of the PxC slab it is possible to decompose the guided photonic modes of the PxC slabs into two non-interacting categories, namely, even and odd modes with respect to the horizontal symmetry plane of the slab [21]. The photonic band structure for the PxC slab structure of Fig. 1(b) for even and odd modes is shown in Fig. 1(d). The normalized radius of the holes and the slab thickness are $r/a = 0.45$, and $d/a = 0.5$, respectively [as in the case of Fig. 1(b)]. Since the photonic modes of the structure are lossy above the light line, only the guided modes that reside below the light line are considered [21]. By comparing Fig. 1(c) and

#123986 - $15.00 USD Received 9 Feb 2010; revised 5 Apr 2010; accepted 7 Apr 2010; published 16 Apr 2010

Fig. 1(d), it can be seen that similar to the phononic case, the photonic bands and therefore, the location and width of the PtBGs, are different for the 2D and 3D cases. By considering Figs. 1(b) and 1(d) it can be seen that a PnBG or even and odd PtBGs simultaneously exist for the square-lattice PxC slab shown in the inset of Fig. 1(b) with geometrical parameters of r/a = 0.45 and d/a = 0.5.

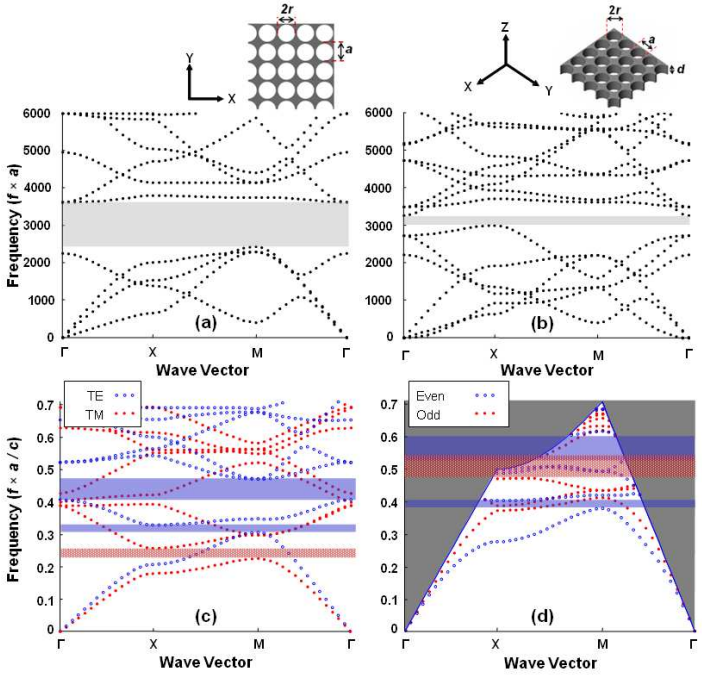

Fig. 1. (a) Band structure of in-plane elastic waves propagating in a 2D square-lattice PnC of infinitely long void holes in Si. A schematic of the cross section of the structures is shown in the inset. In this figure, a is the lattice constant (or distance between the centers of the nearest holes) and r is the radius of the holes. The band structure associates with a structure with r/a = 0.45. (b) Band structure of elastic waves for square lattice of void holes in a Si slab with a finite thickness. A schematic of the structures is shown in the inset, where a is the lattice constant, r is the radius of the holes, and d is the slab thickness. The band structure is calculated for r/a = 0.45 and d/a = 0.5 [14]. (c), (d) Band structure of in-plane-propagating optical modes in the 2D PxC explained in (a) and (b), respectively. The radiation optical modes above the light line are not depicted in (d).

4. Phononic and photonic band gap maps for the square-lattice PxC slab

The demonstration of the simultaneous phononic and photonic band gaps in Fig. 1(b) and Fig. 1(d) necessitates a more detailed analysis to assess the possibility of the existence and the quality of the simultaneous PnBGs/PtBGs in PxC slabs. Phononic and photonic band gap maps for the square-lattice PxC slabs with varying normalized hole radii (r/a) and a fixed normalized thickness of d/a = 0.5 [Fig. 2(a), Fig. 2(c)], and for varying normalized thickness (d/a) and constant normalized hole radii of r/a = 0.45 [Fig. 2(b), Fig. 2(d)] are shown in Fig. 2. Such band gap maps are beneficial for designing PxC slabs with simultaneous PnBG/PtBGs for different applications and conditions.

As shown in Fig. 2(a) for a constant thickness of d/a = 0.5, the PnBG of the square-lattice PxC slab opens up at approximately r/a = 0.43 at frequency of $f \times a$ = 3150 m/s; it widens up as the normalized radius increases. At normalized radius of r/a = 0.49, the PnBG extends to the frequency range of 2170 m/s < $f \times a$ < 3380 m/s. The PnBG map of the same PxC for constant normalized radius of r/a = 0.45 and as a function of the slab thickness is shown in Fig. 2(b). As is visualized in this figure, the PnBGs, opens up at d/a ~0.4 at frequency of 3750

#123986 - $15.00 USD Received 9 Feb 2010; revised 5 Apr 2010; accepted 7 Apr 2010; published 16 Apr 2010

m/s; by increasing the thickness, the PnBG widens up to 2970 m/s < $f \times a$ < 3400 m/s at d/a = 0.55 and closes at d/a = 0.7 at $f \times a$ ~2800 m/s.

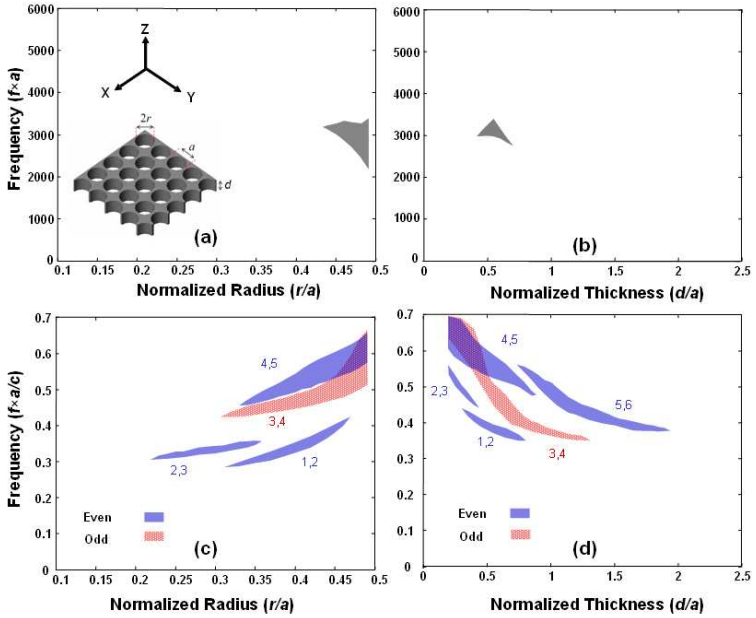

Fig. 2. PnBG maps of the square-lattice PxC slab structure with (a) a constant normalized thickness of d/a = 0.5 as a function of the normalized radius (r/a), and (b) a constant normalized radius of r/a = 0.45 and as a function of normalized thickness (d/a) [14]. (c), (d) PtBG maps of the PxC structure for even and odd optical modes for the same structures as in (a) and (b), respectively. The numbers near each PtBG region show the band numbers between which the PtBGs appear. The schematic of the associated PxC structure is shown in the inset of (a) for reference.

The PtBG map of this PxC for even and odd modes as functions of normalized radius and a constant normalized thickness of d/a = 0.5 is shown in Fig. 2(c). The PtBG maps are calculated considering the band structure of the PtC under the light line of the slab. PtBG regions of narrower than 5% of the center frequency and higher than the sixth band are not considered since such gaps have limitations for realizing practical devices. The band numbers between which each PtBG occurs are shown close to each region. As can be seen in Fig. 2(c), three even PtBGs are present in this PtBG map. The first even PtBG is between 1st and 2nd bands and starts expanding at r/a = 0.33 at $f \times a / c$ = 0.295, where c is the phase velocity of light in vacuum. This even PtBG expands to a PtBG to mid gap ratio (or PtBG ratio) of more than 10% and closes at r/a = 0.47. The second even PtBG occurs between the 2nd and 3rd even bands and opens up at r/a = 0.22 and closes at r/a ~0.36 with a relatively small bandwidth (less than 7% PtBG ratio). Finally, the third even PtBG occurs between the 4th and the 5th bands. It starts at r/a ~0.33 at $f \times a / c$ = 0.465 and expands up to 0.57 < $f \times a / c$ < 0.66 at r/a = 0.49 with a maximum PtBG ratio of approximately 15% at this point. The only present odd PtBG region starts at r/a = 0.3 between the 3rd and 4th odd bands at $f \times a / c$ = 0.42 and expands as the normalized radius increases to r/a = 0.49 at which, 0.51 < $f \times a / c$ < 0.67 with a PtBG ratio of 27%. It is instructive to note that if there are no imperfections in the slab structure, even and odd modes are decoupled from each other and can be separately excited and detected; therefore, several large simultaneous (even or odd) PtBGs and PnBGs can be obtained in this type of PxC for several geometrical parameters.

It is also interesting to note that a PtBG for both even and odd modes also exists in the band structure in Fig. 2(c), which starts at r/a = 0.44 at $f \times a / c$ = 0.52 and expands to 0.57 < f

#123986 - $15.00 USD Received 9 Feb 2010; revised 5 Apr 2010; accepted 7 Apr 2010; published 16 Apr 2010

$\times$ a / c < 0.66 at r/a = 0.49. Interestingly, this common PtBG for even and odd modes overlaps with the PnBG of the PxC at the same range of geometrical parameters. This makes a structure with simultaneous band gaps for all guided optical modes and all elastic waves possible. As an example, for d/a = 0.5 and r/a > 0.45, a PnBG, and PtBGs for both even and odd modes exist. For a PtBG ratio of more than 8% for both even and odd PtBGs, an r/a of 0.47 or larger is required. For r/a = 0.47, to have the center of the PtBG at λ = 1.55μm (i.e., the most desired optical communication wavelength), a and r are calculated to be 890 nm and 418.3 nm, respectively. The spacing between the perimeters of the holes, which is a major parameter dictating the fabrication limitations, is 53.4 nm. This feature size is readily achievable using the advanced fabrication techniques. These geometrical parameters correspond to a PnBG in the frequency range of 2700 m/s < $f \times a$ < 3300 m/s or 3 GHz < f < 3.7 GHz (a PnBG ratio of 21%), and PtBG ratios of 19% and 13% for the individual even and odd PtBGs, respectively.

The PtBG maps of this structure for a constant normalized radius of r/a = 0.45 and variable d/a are also shown in Fig. 2(d) confirming the existence of the simultaneous PtBGs and PnBGs in the square-lattice PxC slabs.

5. Phononic and photonic band gap maps for the triangular-lattice PxC slab

According to the large PtBGs that can be obtained in moderate void to solid ratios in triangular-lattice PxC slabs, these structures are of great interest in realizing photonic crystal devices [2, 3, 21]; therefore, it is important to evaluate their phononic characteristics for obtaining simultaneous PnBGs and PtBGs. To attain PnBGs in the triangular PxC slabs of cylindrical holes in a slab, we simulated the structure for a variety of geometrical parameters; however, through our extensive search, we were unable to obtain a sizable PnBG in this lattice. We analyzed the structures for radius of holes in the range 0.1 < r/a < 0.49 with a step size of 0.02 and for each normalized radius we calculated the PnBG in the normalized thickness range of 0.1 < d/a < 2, with a 0.1 step size. However, no sizable PnBG was obtained for this structure despite our extensive simulations. The PtBG maps of the triangular-lattice PxC slab have already been extensively studied before [23], and will not be repeated here since no PnBG could not be obtained.

6. Phononic and photonic band gap maps for the hexagonal-lattice PxC slab

Compared with the square-lattice PxC slab structures, hexagonal-lattice structures are more desirable for phononic applications as they can provide larger PnBGs with more relaxed fabrication limitations [14]. As will be shown below, simultaneous PnBGs and PtBGs for both even and odd modes can also be obtained in the hexagonal lattice.

The PnBG and PtBG maps for the hexagonal-lattice PxC slab structure are shown in Fig. 3(a)-(d). The calculations have been performed using the developed PWE tool. The schematic of the analyzed hexagonal-lattice PxC slab structure is shown in the inset of Fig. 3(a) where geometrical parameters of the structure are indicated. In this schematic, a is the distance between the centers of the two nearest holes, d is the thickness of the slab, and r is the radius of the holes. The PnBG map for varying radius of the holes with a constant thickness of d/a = 1 is shown in Fig. 3(a). The PnBG map is also derived for a varying slab thickness and a constant normalized radius of r/a = 0.45 in Fig. 3(b). These values for the normalized radius and thickness are chosen as they can attain large PnBGs. The PnBG for this PxC slab structure of d/a = 1 opens up at r/a = 0.36 and expands as the normalized radius increases. As shown in Fig. 3(b), four different regions of PnBGs exist in the PnBG map. The range of geometrical parameters of the hexagonal-lattice PxC required for achieving PnBGs corresponds to values that are more practical from the structure stability and fabrication points of view compared to the square-lattice PxCs.

#123986 - $15.00 USD Received 9 Feb 2010; revised 5 Apr 2010; accepted 7 Apr 2010; published 16 Apr 2010

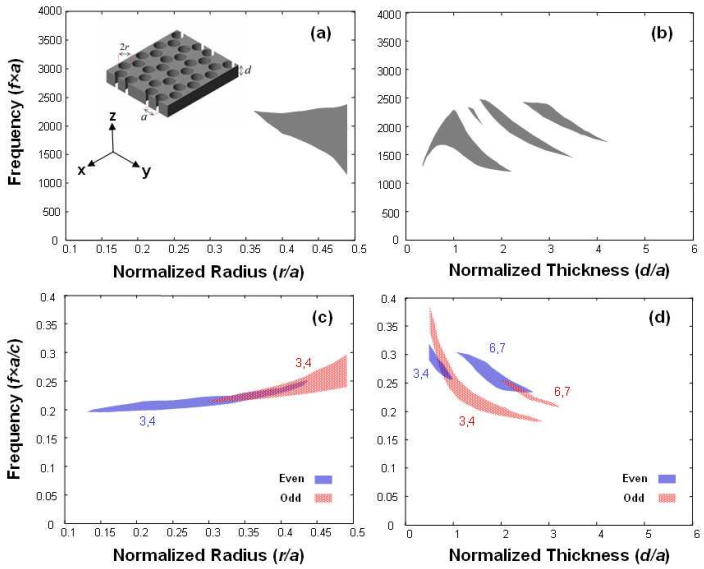

Fig. 3. PnBG maps of the hexagonal-lattice PxC slab structure with (a) a constant normalized thickness of d/a = 1 as a function of the normalized radius (r/a) and (b) a constant normalized radius of r/a = 0.45 and as a function of the normalized slab thickness (d/a) [14]. (c), (d) PtBG maps of the PxC structure for even and odd optical modes for the same geometrical parameters as in (a) and (b), respectively. The numbers near each PtBG region show the band numbers between which the PtBGs appear. The schematic of the hexagonal PxC structure is shown in the inset of (a) for reference.

We also analyzed the photonic band structure of the hexagonal-lattice PxC slab shown in Fig. 3(a) using 3D PWE. In our calculations, PtBGs that occur at frequencies higher than the 7th band in the band structures are not considered due to practical considerations. Figures 3(c) and 3(d) show the PtBG of the hexagonal lattice for the same range of geometrical parameters associated with Figs. 3(a) and 3(b), respectively. Similar to the case for the square-lattice PxC, the band numbers between which each PtBG occurs are shown next to each PtBG. As can be seen from Fig. 3(c), both even and an odd PtBGs are supported for a wide range of geometrical parameters of this structure. The even and odd PtBG regions overlap over the normalized radius range of $0.29 < r/a < 0.42$. However, the PtBG ratio of this overlapping PtBG region is limited to about 5%, which may not be sufficient for wide-band applications; rather, the PtBG of the odd modes can be made large enough by increasing the normalized radius and can be used for many of the envisioned applications.

As a practical example, an odd PtBG ratio of 12% ($0.226 < f \times a/c < 0.254$) can be obtained for r/a = 0.42 and d/a = 1, at which the PnBG is obtained in frequency range of 1780 m/s $< f \times a <$ 2249 m/s (~23%), which is appropriate for wide bandwidth applications of PxC structures. For λ = 1.55 μm, the required value of a would be 371.2 nm, which corresponds to a center phonon frequency of 5.4 GHz. Other parameters of this structure are r = 155.9 nm, d = 371.2 nm, and spacing between hole perimeters of 59.4 nm, which falls into practical fabrication conditions. Such geometrical parameters impose similar fabrication limitations compared to the square-lattice PxCs; however, due to a smaller volume ration of void compared to the square lattice, the hexagonal lattice can have a better mechanical stability.

Figure 3(d) shows the PtBG maps of the PxC as a function of the thickness of the slab for a constant normalized radius of r/a = 0.45. There are four regions (two odd and two even) of PtBG in Fig. 3(d). The band numbers between which the PtBGs are formed are also indicated in this figure. As can be seen by comparing Fig. 3(b) and Fig. 3(d), simultaneous PnBGs and either even or odd PtBGs exist for several values of d/a; Therefore, based on the intended

#123986 - $15.00 USD Received 9 Feb 2010; revised 5 Apr 2010; accepted 7 Apr 2010; published 16 Apr 2010

applications, any of such simultaneous band gaps can be utilized. As can be seen in Fig. 3(d), there are two common even and odd PtBG regions. Both of these regions have PtBG ratios of less than 5%, which may be too small for some of the envisioned applications.

7. Comparison of the structures

The results presented show that both square and hexagonal-lattice PxC structures of void cylindrical holes embedded in a solid slab are appropriate for achieving simultaneous band gaps for phonons and photons. As can be inferred from the two given examples, for a certain optical wavelength, both lattice types impose similar fabrication limitations while the hexagonal lattice may benefit from a better mechanical stability. If the PtBG is required to exist for both even and odd symmetries simultaneously with PnBGs, then square-lattice PxCs are favorable. Despite our extensive search for PnBGs, no PnBGs could be obtained in the triangular-lattice PxC slab. It should also be noted that in this paper only the complete PnBGs were considered due to the full control they can provide over elastic vibrations. If PnBGs of certain symmetry (e.g. even or odd) in PxC slabs are also of interest, the range of geometrical parameters with simultaneous PtBGs and PnBGs can be expanded compared to what reported here.

8. Concluding remarks

In this paper, we theoretically demonstrate phoxonic crystal (PxC) slab structures that can provide simultaneous photonic and phononic band gaps at optical communication wavelengths and acoustic frequencies of a few GHz. We analyzed PxCs made of the most highly used (square, hexagonal, and triangular) 2D arrays of void cylindrical holes in a Si slab and showed that large simultaneous PnBGs/PtBGs can be obtained for both square and hexagonal-lattice arrangement of holes but not for the triangular-lattice arrangement. We showed that the PtBGs and PnBGs in PxC slabs (calculated using 3D simulations) are different compared to the PnBG and PtBGs of the previously reported 2D PxCs with infinite thickness (calculated using 2D simulations). For a certain optical wavelength and similar band gap ratios, we showed that both square and hexagonal-lattice PxC slab structures impose similar fabrication limitations while the hexagonal lattice can provide better mechanical stability. We further have shown that simultaneous PnBGs and PtBGs for both odd and even modes can be obtained in both hexagonal and square-lattice PxC slab structures while the square-lattice PxC is advantageous. We believe the results presented in this paper can lead to structures that can greatly enhance opto-mechanical and acousto-optic interactions that require simultaneous localization of photonic and elastic waves.

Acknowledgements

This work was supported by the Office of Naval Research under Contract No. 21066WK (M. Spector).

#123986 - $15.00 USD Received 9 Feb 2010; revised 5 Apr 2010; accepted 7 Apr 2010; published 16 Apr 2010